# Automobile Design Using the *GENESIS* Structural Optimization Program

Juan Pablo Leiva, Liangsheng Wang, Sebastien Recek and Brian C. Watson

Vanderplaats Research & Development, Inc.
1767 South 8th Street, Suite 100, Colorado Springs, CO 80906, USA
e-mail: jp@vrand.com - phone: (719) 473-4611

## Abstract

*This paper describes the use of the GENESIS program to solve structural optimization problems in automobile design. A brief description of the GENESIS program and the technology behind it is presented. Studies that help designers with maximizing frequencies and finding the best locations for welds are described. Studies on optimization of composite materials are also covered.*

## 1. Introduction

Often automobile engineers need to decide where to reinforce their designs to improve some attributes. After deciding where to reinforce, they also need to know how much material to allocate to the reinforcement. This paper discusses these two issues. A study on how to define the optimal location of material is discussed. A novel idea for that purpose is presented and it is used with topology optimization to solve example problems. The "how much material to allocate" problem is discussed and example problems are presented using sizing optimization to find the optimal thicknesses of layers and the optimal fiber orientations of composite materials. Another common problem engineers face is where to locate welds to maintain the rigidity of their design. In this paper, this problem is also discussed and examples using sizing optimization are provided.

## 2. The GENESIS Program and the Technology Behind It

The GENESIS program is a software that allows the user to solve static, inertia relief, buckling, normal modes, direct frequency response, modal frequency response and heat transfer analysis problems. GENESIS can solve sizing, shape and topology optimization problems. The topology optimization capabilities are typically used for creating preliminary designs while the shape and sizing optimization capabilities are normally used to obtain detailed or final designs [1].

The GENESIS program fully integrates optimization with finite element analysis. For shape and sizing optimization GENESIS uses the latest approximation concepts available. Schmit and co-workers introduced approximation concepts in the 1970s [2,3], and enhancements to response approximations were introduced in the 1980s [4,5,6]. The high quality approximations used in GENESIS are able to capture the important physics of the structural optimization problem, substantially reducing the cost of performing multiple finite element analyses. GENESIS typically can find an optimal solution in ten or fewer full-system finite element analyses for almost any type of structural problem with many kinds of structural responses [7]. Advances in the computer industry have also made possible the solution of very large problems, consisting of millions degrees of freedoms with of thousands of design variables and millions of constraints. Occasionally the problems contain tens of thousands of design variables.

In topology optimization, GENESIS also uses approximation concepts [8]. The cost of solving the topology optimization problem is normally higher than in shape and sizing optimization due to the increased complexity of the problem. GENESIS, in this case, typically converges in 15 to 25 design cycles. GENESIS topology optimization is based on the density method [9]. GENESIS uses the DOT [10] or the BIGDOT [11] optimizers to solve the approximate optimization problems.

## 3. Automobile Applications Using GENESIS

Automobile applications of structural optimization are numerous. Today almost any structural part of an automobile can be optimized using GENESIS. Examples of small parts such as mirrors, steering knuckles, rocker panels, mounting brackets, pillars, seat frames, trunk reinforcements, suspension rings and tie rods or large parts such as engine blocks, chassis and whole car bodies, can be found in the literature. See for examples references [12-17].

## 4. Stiffness Optimization of a Car Body Using Topology Optimization

Topology optimization is typically used to find the optimal distribution of material in a given designable region that meets a predefined criterion. With topology optimization, designable regions of the structure that have the least contribution to the overall stiffness or natural frequency are identified. This tells which regions should be removed from the structure to minimize the mass while having the least impact on the performance of the structure. After the topology optimization is finished, the analysis model may be re-built by taking out the elements that topology has indicated to be unnecessary, and sizing and or shape optimization may be performed to refine the solution.
Where to reinforce a car body is a good example of the use of topology optimization. In the following example, a novel method is presented. The method has two simple steps. The first step consists in adding a second layer of elements on areas where it is possible to reinforce. The second step consists of the topology optimization of the second layer to find out which areas of the second layer should be kept or which areas are not important and should not be considered for reinforcement.

### 4.1 Problem Description

To illustrate this method, a finite element mesh of a Porsche 928 car body is optimized for three different objective functions. The first objective is to maximize the first bending frequency of the car; the second objective is to maximize the first natural torsional frequency of the car; and finally the third objective function is to maximize the average of the first natural bending frequency and the first natural torsional frequency. Three different mass constraints were used in each of the optimization studies (2.0%, 5.0% and 10% of added material). Mode tracking was used in all 9 studied cases to make sure that the final mode numbers matched the physical modes of interest. The second layer added covers the whole car body and its thickness is 1mm and is of steel material.

Table 1 shows a summary of selected items of the finite element model of the original model and the topology optimization model with the second layer of elements. The overlapped second layer of shell elements contained 34560 QUAD4 and TRIA3 elements.

Table 2 shows the results of the eigenvalue analysis of the original design and the model with two layers with uniformly distributed mass. The first natural torsion frequency mode is No. 9 and the corresponding frequency is 31.947 Hz. The first natural bending mode is No.18 and the corresponding frequency is 46.132 Hz. Table 2 also shows that the lowest natural frequencies have decreased a little after adding a shell sheath, which indicates that distributing the extra mass evenly may not increase the rigidity of the car body relative to the increased mass. The model used did not include the engine mass, the door, the glasses and other structural components.

| Item | Original Model | Sheath-added Model |
|---|---|---|
| Number of Grid Points | 27252 | 27252 |
| Number of CQUAD4 Elements | 22072 | 44144 |
| Number of CTRIA3 Elements | 12488 | 24976 |
| Number of degrees of freedom | 163512 | 163512 |
| Number of designable elements | - | 34560 |
| Number of design variables | - | 34560 |

**Table 1. Summary of Finite Element Models**

| No. | Original Model | | Shell Sheath-added Model (Initial results) | |
|---|---|---|---|---|
| | Frequency (Hz) | Mode Type | Frequency (Hz) | Mode Type |
| 1 | 0.0 | Rigid | 0.0 | Rigid |
| 2 | 0.0 | Rigid | 0.0 | Rigid |
| 3 | 0.0 | Rigid | 0.0 | Rigid |
| 4 | 0.0 | Rigid | 0.0 | Rigid |
| 5 | 0.0 | Rigid | 0.0 | Rigid |
| 6 | 0.0 | Rigid | 0.0 | Rigid |
| 7 | 27.369 | Local 1 | 27.369 | Local 1 |
| 8 | 27.482 | Local 2 | 27.481 | Local 2 |
| 9 | 31.947 | Natural torsion 1 | 31.940 | Natural torsion 1 |
| 10 | 37.083 | Local 3 | 37.083 | Local 3 |
| 11 | 37.481 | Natural torsion 2 | 37.481 | Natural torsion 2 |
| 12 | 39.217 | Natural torsion 3 | 39.220 | Natural torsion 3 |
| 13 | 41.999 | Local 4 | 41.997 | Local 4 |
| 14 | 42.456 | Local 5 | 42.457 | Local 5 |
| 15 | 42.886 | Local 6 | 42.828 | Local 6 |
| 16 | 43.872 | Local 7 | 43.872 | Local 7 |
| 17 | 45.419 | Natural torsion 4 | 45.426 | Natural torsion 4 |
| 18 | 46.137 | Natural bending 1 | 45.927 | Natural bending 1 |

**Table 2. Vibration Modes**

Figure 1 shows an example of a first natural bending mode.

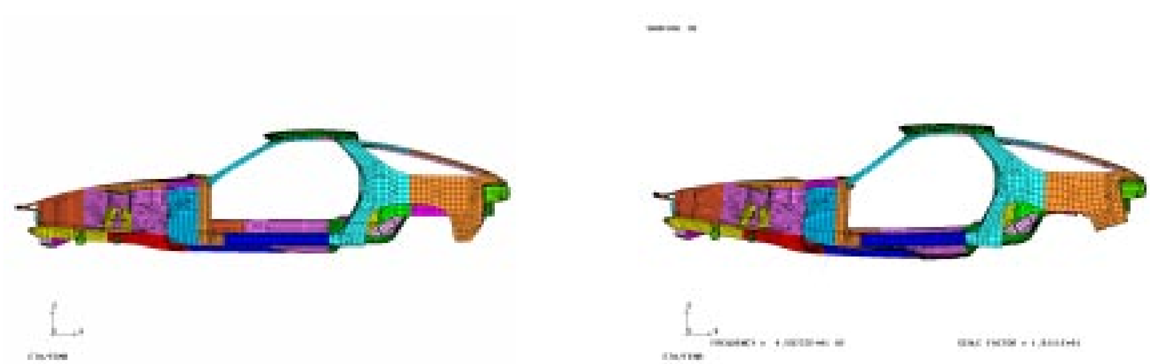

**Figure 1. First Natural Bending mode**

Figures 2 shows an example of a first natural torsional mode.

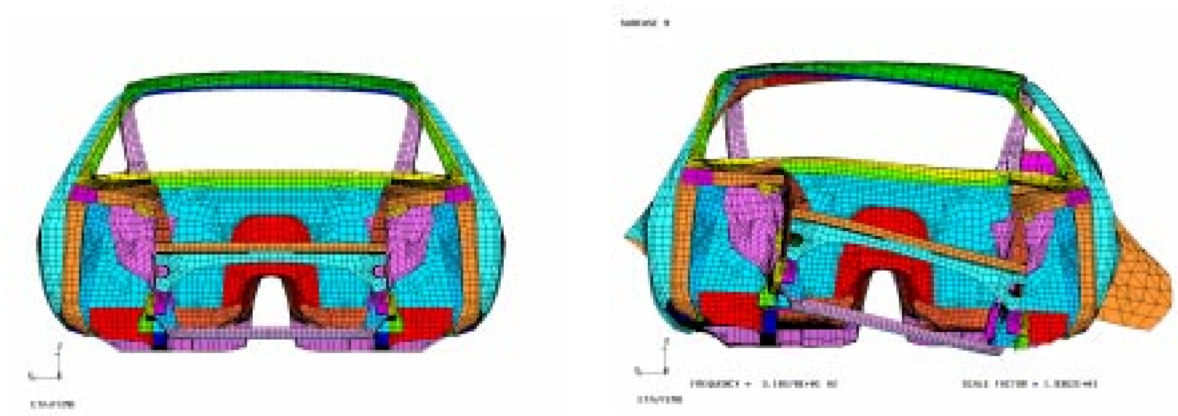

**Figure 2. First Natural Torsional Mode**

### 4.2 First Bending Maximization Problem

The objective in this case is to maximize the first bending frequency of the car. Three different mass constraints were used in each of the optimization studies (2.0%, 5.0% and 10% of added material). Figure 3 shows in dark (red) the optimal locations to reinforce the car body. The results shown correspond to the case where the reinforcement can be up to 7.8kg (5.0% of additional mass).

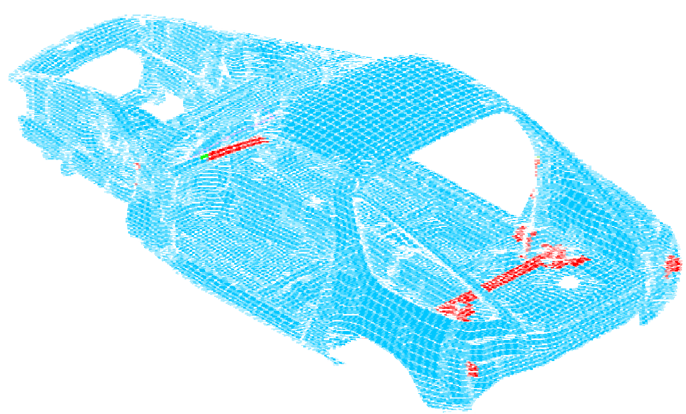

**Figure 3. First Natural Bending Maximization Results**

### 4.3 First Torsional Maximization Problem

The objective in this case is to maximize the first torsional frequency of the car. Three different mass constraints were used with this optimization objective (2.0%, 5.0% and 10% of added material). Figure 4 shows in dark (red) the optimal locations to reinforce the car body. The results shown correspond to the case where the reinforcement can be up to 7.8kg (5.0% of additional mass).

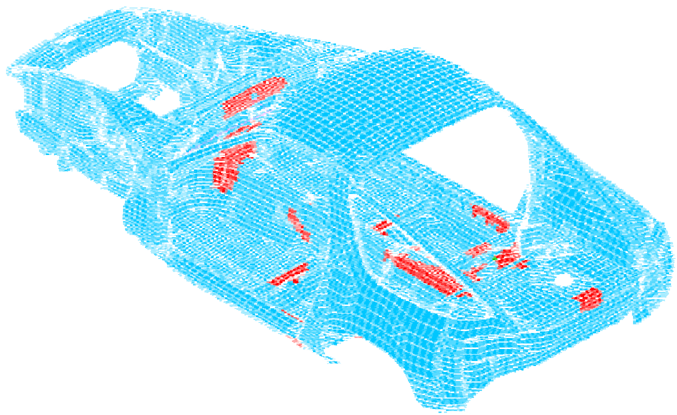

**Figure 4. First Torsion Maximization Results**

### 4.4 Average of First Torsion and First Bending Frequencies Maximization Problem

The objective in this case is to maximize the average of the first bending and first torsional frequency of the car. Three different mass constraints were used with this optimization objective (2.0%, 5.0% and 10% of added material). Figure 5 shows in dark (red) the optimal locations to reinforce the car body. The results shown correspond to the case where the reinforcement can be up to 7.8kg (5.0% of additional mass).

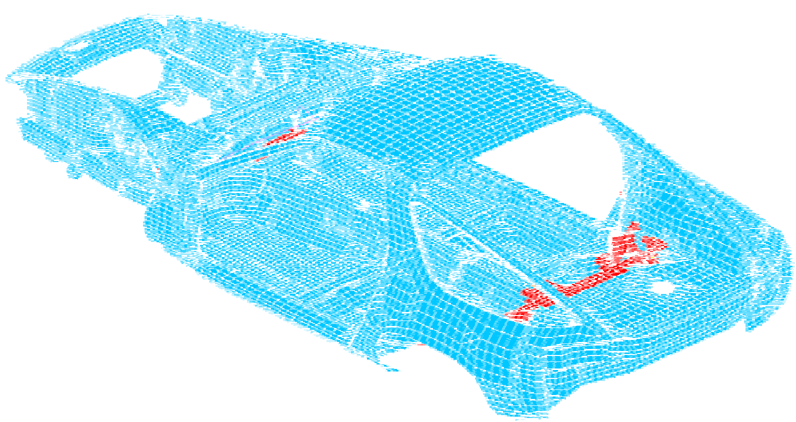

**Figure 5. Average of First Torsion and First Bending Frequencies Maximization Results**

### 4.5 Summary and Commentaries of Topology Optimization Results

Table 3 shows the relation between increased frequencies and added mass optimization for all nine studies.

| Added Mass (Kg) | Increased Frequency (Hz) | | |
|---|---|---|---|
| | Maximizing 1st Torsion Frequency | Maximizing 1st Bending Frequency | Maximizing Average of Two Frequencies |
| 3.11 | 0.19 | 0.89 | 0.42 |
| 7.78 | 0.83 | 1.84 | 1.31 |
| 15.57 | 2.15 | 3.43 | 3.34 |

**Table 3. Relation Between Increased Frequency and Added Mass**

Figure 6 shows in a graph the relation between increased frequencies and added mass optimization for all nine studies.

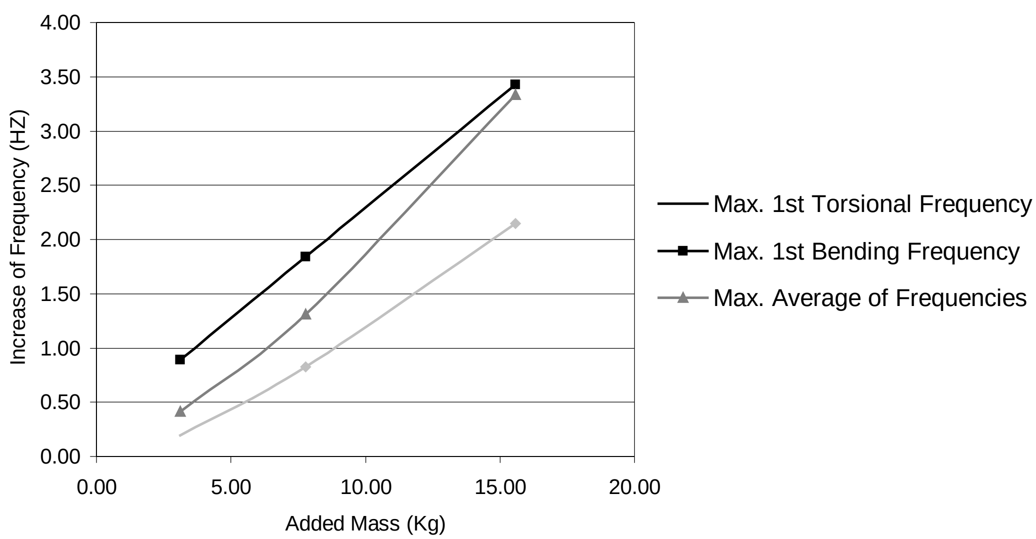


**Figure 6. Relation Between Increased Frequency And Added Mass**

The different results of rigidity optimization show that different distributions of added mass could bring about different results. Optimal distribution of added mass can obtain the highest rigidity. Otherwise the rigidity may not increase and even may decrease greatly.

This study shows that topology optimization can efficiently give insight on where to add material and how much to add in order to improve the performance of the car body.

Car bodies can be reinforced according to the results of topology optimization. In the next examples, this topology results are used.

## 5. Stiffness Optimization of a Car Body Using Sizing Optimization

Existing car body designs can be improved using reinforcement patches manufactured with layered composite materials. The proper dimension of each layer of the composite material as well as the orientation of the fiber can be found using sizing optimization.

In this study, a model of a Porsche 928 is used to illustrate the technique. The model is optimized for the same three objective functions used in the previous section. The first objective is to maximize the first bending frequency of the car, the second objective is to maximize the first natural torsional mode of the car, and finally the third objective function is to maximize the average of the first natural frequency and the first natural torsional frequency. For each optimization case, two different mass constraints were used (5 kg and 10kg). Mode tracking was used in all 6 cases to make sure that the final mode numbers matched the physical modes of interest.

The composite patches are added on the car body model in places indicated by the topology optimization results. These patches will modify the mass distribution of the car body. The material chosen for the patches is carbon-epoxy. The patches are placed on the steel body using glue. A new round of optimization is required to determine the optimal thickness of each layer and angle of the fibers in each layer.

Table 4 summarizes the properties of the composite material.

| | |
|---|---|
| Young Modulus in fiber's direction | **51GPa** |
| Young Modulus in fiber's perpendicular direction | **18GPa** |
| Poisson's ratio | **0.25** |
| Density | **1400kg/m$^3$** |

**Table 4. Composite Material Properties**

Four layers composite patches where chosen. Therefore, there are eight design variables per patch. To simplify the model, the glue thickness is ignored. Figure 7 shows the section of a typical patch.

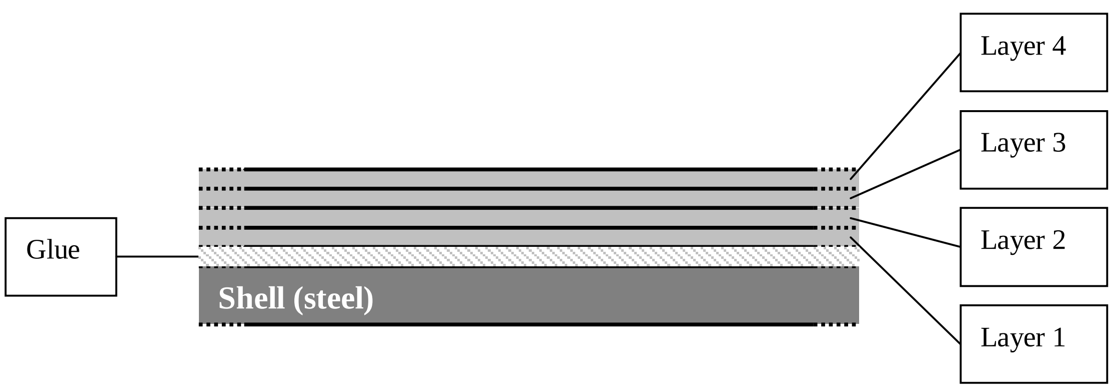


**Figure 7. Section of a Patch**

Two sets of different groups of patches were used. One set was used for the bending and for the average optimization, and a second set was used for the torsional optimization. The angles for the fibers are taken with respect to the longitudinal direction of the car, except for the pillars where they were taken with respect to the longitudinal direction of each pillar.

### 5.1 Bending Stiffness Optimization Using Sizing Optimization

The objective of this problem was to maximize the first bending natural frequency. Two cases are considered; in the first case only 5kg could be added. In the second case 10kg could be added. Five patches were used. In each patch, 4-thickness design variables and 4 angle design variables were used for a total of 40 design variables.

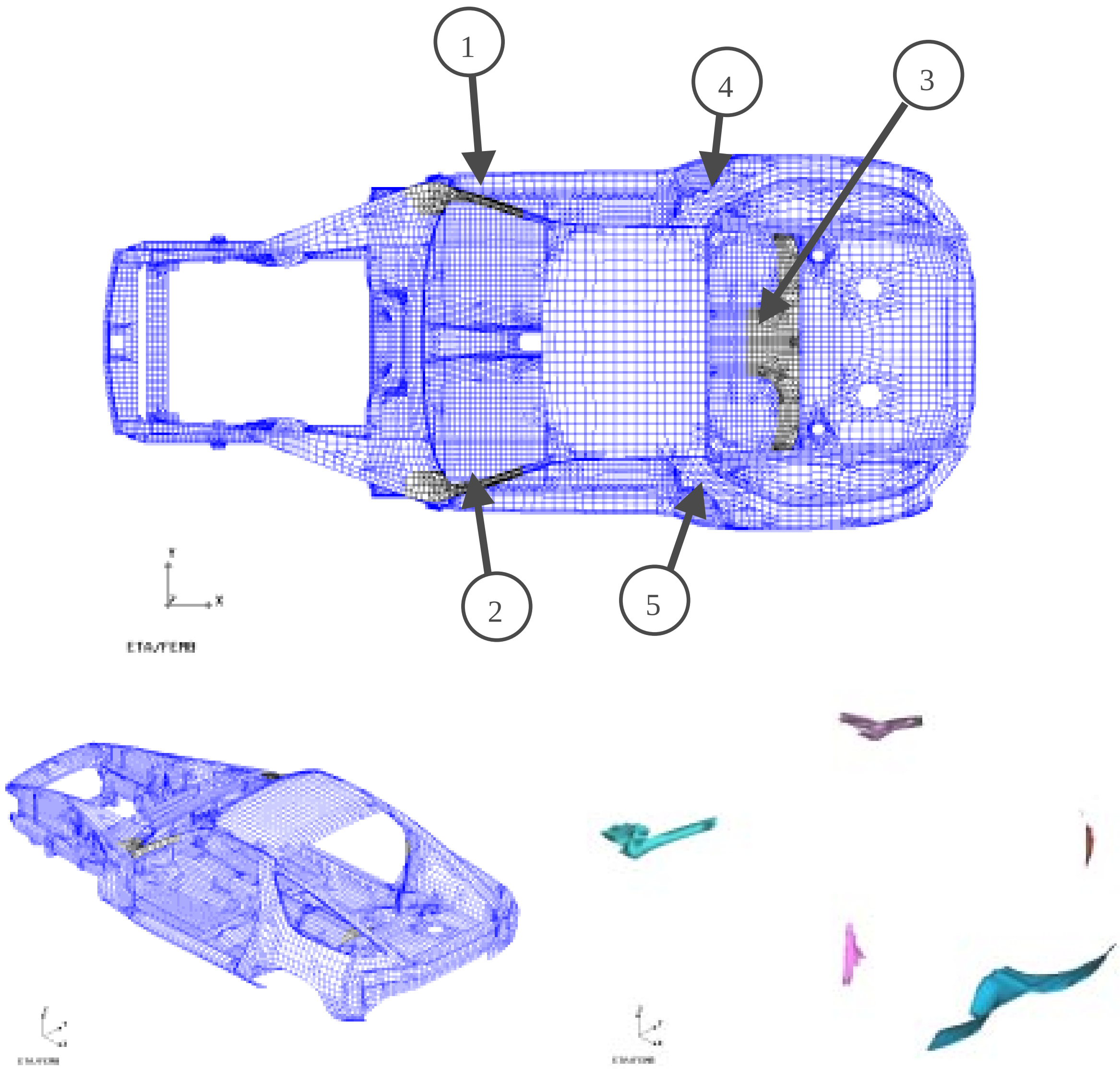


**Figure 8. Patches for First Bending Frequency Optimization**

Tables 5a and 5b show the results of the two-optimization runs. From these tables, it can be seen that the first bending frequency was increased by 4.25 Hz and 7.02 Hz on the first and second run respectively. The tables also show that the first torsional frequency increased by 0.94 Hz in the first run and 1.21 Hz for the second. The average of the first natural bending frequency and the first natural torsion frequency increased by 2.59 Hz in the first run, and 4.12 Hz on the second run.

| | 5kg added | | | | | | | | | |
|---|---|---|---|---|---|---|---|---|---|---|
| | PATCH 1 | | PATCH 2 | | PATCH 3 | | PATCH 4 | | PATCH 5 | |
| | Thickness | Angle | Thickness | Angle | Thickness | Angle | Thickness | Angle | Thickness | Angle |
| Layer 4 | 1.59 | -8.65 | 1.57 | 4.25 | 1.74 | -9.00 | 1.20 | -90.00 | 1.30 | -45.00 |
| Layer 3 | 1.79 | 0.00 | 1.70 | 0.00 | 1.42 | -90.00 | 0.97 | -82.35 | 1.06 | 90.00 |
| Layer 2 | 1.79 | 0.00 | 1.70 | -3.26 | 1.42 | 39.91 | 0.96 | 12.00 | 1.12 | 90.00 |
| Layer 1 | 1.65 | -4.25 | 1.55 | -4.25 | 1.62 | 42.19 | 1.19 | 45.00 | 1.33 | 90.00 |
| | **Increase of the average of the first torsion and bending frequencies** | | | | | | | | **2.591895 Hz** | |
| | **Increase of the first torsion frequencies** | | | | | | | | **0.93746 Hz** | |
| | **Increase of the first bending frequencies** | | | | | | | | **4.24633 Hz** | |

| | 10kg added | | | | | | | | | |
|---|---|---|---|---|---|---|---|---|---|---|
| | PATCH 1 | | PATCH 2 | | PATCH 3 | | PATCH 4 | | PATCH 5 | |
| | Thickness | Angle | Thickness | Angle | Thickness | Angle | Thickness | Angle | Thickness | Angle |
| Layer 4 | 3.23 | 9.58 | 2.96 | -1.08 | 3.74 | -56.25 | 2.22 | -90.00 | 2.37 | -84.38 |
| Layer 3 | 3.30 | 2.50 | 2.99 | 2.50 | 3.13 | -50.14 | 1.93 | 1.93 | 2.06 | 8.65 |
| Layer 2 | 3.30 | 2.50 | 2.99 | 2.50 | 3.13 | -50.14 | 1.93 | -45.14 | 2.06 | 19.64 |
| Layer 1 | 3.25 | 1.08 | 2.94 | 1.08 | 3.42 | 50.63 | 2.30 | 67.50 | 2.44 | 84.38 |
| | **Increase of the average of the first torsion and bending frequencies** | | | | | | | | **4.118745 Hz** | |
| | **Increase of the first torsion frequencies** | | | | | | | | **1.21449 Hz** | |
| | **Increase of the first bending frequencies** | | | | | | | | **7.023 Hz** | |

**Table 5a and 5b. Results For First Bending Frequency Maximization (thickness in mm, angle in °)**

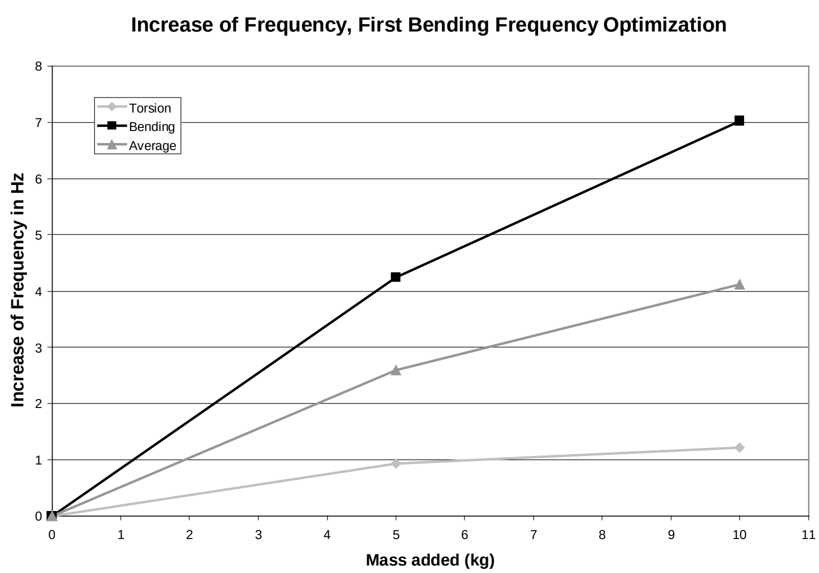


**Figure 9. Frequency Increases for Different Mass Constraints**

### 5.2 Torsional Stiffness Optimization Using Sizing Optimization

The objective of this problem was to maximize the first torsional natural frequency. Two cases are considered; in the first case only 5kg could be added. In the second case, 10kg could be added. Six patches were used. In each patch, 4-thickness design variables and 4 angle design variables were used for a total of 48 design variables.

Patch 1 is used to reinforce the bottom of the windshield frame, the patch 2 is used to reinforce the rear of the car, the patch 3 reinforces the floor and the transmission axle tunnel, patches 4 and 5 reinforce the bottom of the door's frame and the patch 6 reinforces the front of the transmission tunnel (under the patch 1).

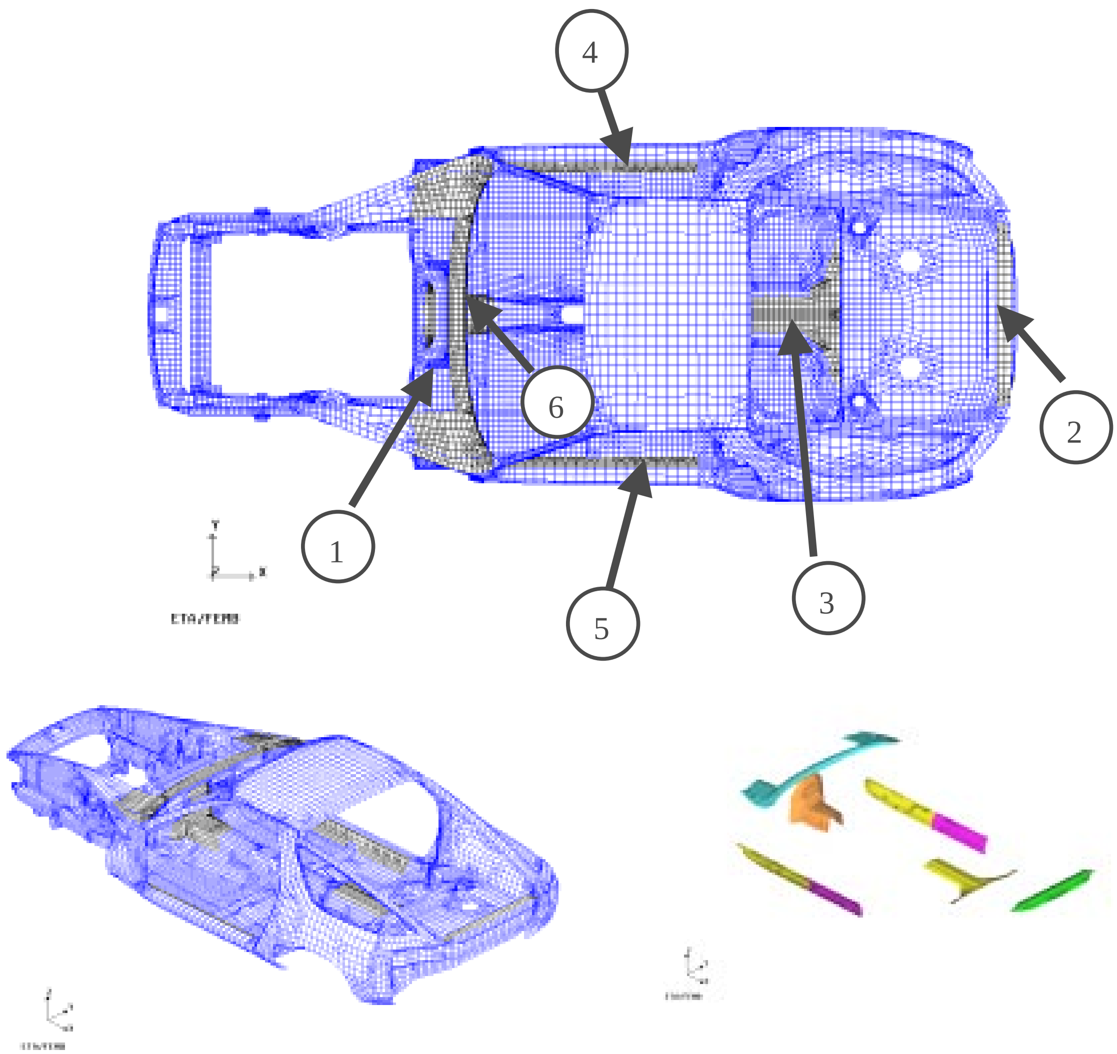


**Figure 10. Patches for First Torsion Frequency Optimization**

Tables 6a and 6b show the results of the two-optimization runs. From these tables, it can be seen that the first torsional frequency was increased by 2.09 Hz and 2.64 Hz on the first and second run respectively. The tables also show that the first bending frequency increased by 1.44 Hz in the first run and 2.40 Hz for the first for the second. The average of the first natural bending frequency and the first natural torsion frequency increased by 1.76 Hz, in the first run and, 2.52 Hz on the second.

| | 5kg added | | | | | | | | | |
|---|---|---|---|---|---|---|---|---|---|---|
| | **PATCH 1** | | **PATCH 2** | | **PATCH 3** | | **PATCH 4&5** | | **PATCH 6** | |
| | Thickness | Angle | Thickness | Angle | Thickness | Angle | Thickness | Angle | Thickness | Angle |
| Layer 4 | 2.71 | 92.47 | 0.03 | 43.60 | 0.97 | 90.23 | 0.00 | 0.66 | 0.37 | 6.10 |
| Layer 3 | 1.34 | 3.99 | 0.02 | -19.46 | 0.95 | 0.36 | 0.02 | -0.07 | 0.37 | -8.49 |
| Layer 2 | 1.34 | -3.98 | 0.02 | -22.23 | 0.95 | 0.97 | 0.00 | -0.30 | 0.37 | 59.96 |
| Layer 1 | 2.94 | -91.54 | 0.04 | -64.56 | 0.93 | 0.09 | 0.00 | 0.26 | 0.43 | -95.14 |
| | **Increase of the average of the first torsion and bending frequencies** | | | | | | | | **1.76383** | **Hz** |
| | **Increase of the first torsion frequencies** | | | | | | | | **2.09211** | **Hz** |
| | **Increase of the first bending frequencies** | | | | | | | | **1.43555** | **Hz** |

| | 10kg added | | | | | | | | | |
|---|---|---|---|---|---|---|---|---|---|---|
| | **PATCH 1** | | **PATCH 2** | | **PATCH 3** | | **PATCH 4&5** | | **PATCH 6** | |
| | Thickness | Angle | Thickness | Angle | Thickness | Angle | Thickness | Angle | Thickness | Angle |
| Layer 4 | 4.00 | 91.34 | 0.26 | 30.65 | 2.20 | 125.46 | -0.01 | -0.31 | 0.94 | 4.55 |
| Layer 3 | 3.33 | 7.36 | 0.21 | -37.96 | 2.38 | 25.87 | 0.01 | -0.03 | 0.98 | -9.36 |
| Layer 2 | 3.34 | -15.21 | 0.21 | -52.57 | 2.38 | 5.72 | 0.01 | 0.14 | 0.98 | -72.07 |
| Layer 1 | 4.00 | -85.14 | 0.27 | -95.72 | 2.37 | -14.90 | 0.01 | 0.01 | 1.01 | -116.05 |
| | **Increase of the average of the first torsion and bending frequencies** | | | | | | | | **2.52176** | **Hz** |
| | **Increase of the first torsion frequencies** | | | | | | | | **2.64007** | **Hz** |
| | **Increase of the first bending frequencies** | | | | | | | | **2.40345** | **Hz** |

**Tables 6a and 6b. Results for First Torsion Frequency Maximization (thickness in mm, angle in °)**

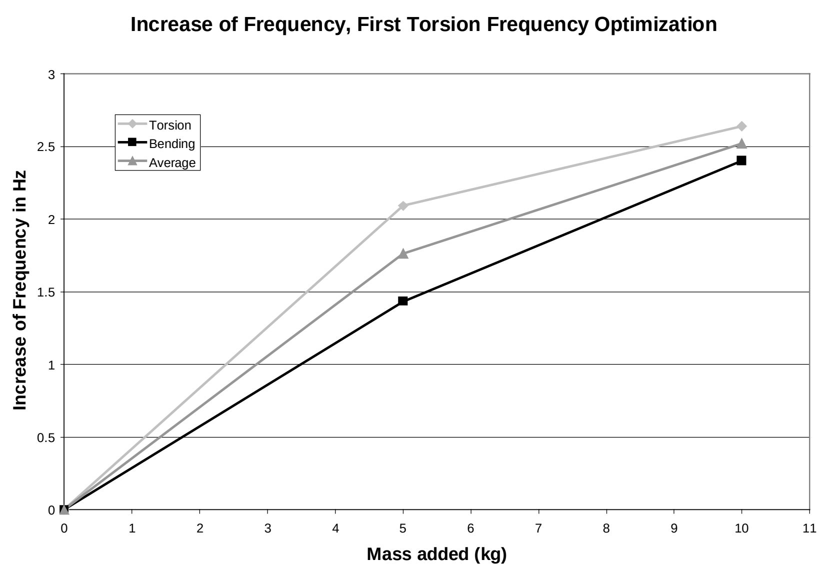


**Figure 11. Frequency Increases for Different Mass Constraints**

### 5.3 Average of Bending and Torsion Frequency Optimization Using Sizing Optimization

The objective of this problem was to maximize the average of the sum of the first bending natural frequency and the first torsional natural frequency. Two cases are considered; in the first case only 5kg could be added. In the second case 10kg could be added. The same five patches used in the bending optimization problem were used, so here also 40 design variables were used.

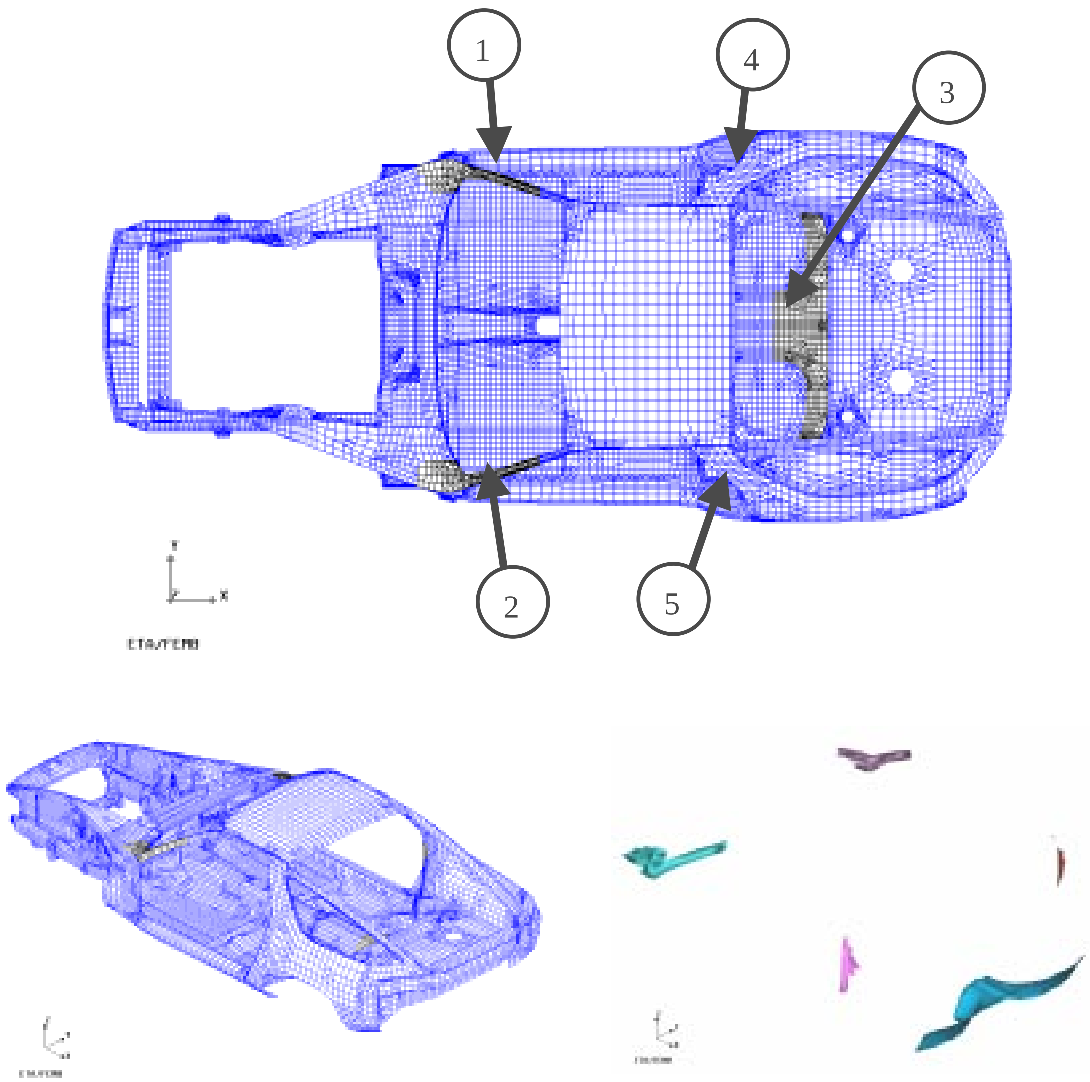


**Figure 12. Patches for First Torsion Frequency Optimization**

Tables 7a and 7b show the results of the two-optimization runs. From these tables, it can be seen that the average of first bending frequency and first torsional frequency was increased by 2.60 Hz and 4.09 Hz on the first and second run respectively. The tables also shown that the first bending frequency increased by 4.25 Hz in the first run and 6.96 Hz for the first for the second. The first natural torsion frequency increased by 0.95 Hz, in the first run, and 1.22 Hz on the second run.

| | 5kg added | | | | | | | | | |
|---|---|---|---|---|---|---|---|---|---|---|
| | PATCH 1 | | PATCH 2 | | PATCH 3 | | PATCH 4 | | PATCH 5 | |
| | Thickness | Angle | Thickness | Angle | Thickness | Angle | Thickness | Angle | Thickness | Angle |
| Layer 4 | 1.69 | 4.25 | 1.65 | 4.25 | 1.62 | -67.50 | 1.10 | -90.00 | 1.14 | -67.50 |
| Layer 3 | 1.83 | 0.00 | 1.76 | 0.00 | 1.39 | -31.48 | 0.86 | -31.48 | 0.97 | 27.57 |
| Layer 2 | 1.83 | 0.00 | 1.76 | 0.00 | 1.39 | -31.48 | 0.86 | -9.74 | 0.97 | 31.48 |
| Layer 1 | 1.71 | -4.25 | 1.63 | -4.25 | 1.59 | 75.94 | 1.02 | 69.07 | 1.32 | 90.00 |
| | **Increase of the average of the first torsion and bending frequencies** | | | | | | | | **2.60185** | **Hz** |
| | **Increase of the first torsion frequencies** | | | | | | | | **0.94959** | **Hz** |
| | **Increase of the first bending frequencies** | | | | | | | | **4.25411** | **Hz** |

| | 10kg added | | | | | | | | | |
|---|---|---|---|---|---|---|---|---|---|---|
| | PATCH 1 | | PATCH 2 | | PATCH 3 | | PATCH 4 | | PATCH 5 | |
| | Thickness | Angle | Thickness | Angle | Thickness | Angle | Thickness | Angle | Thickness | Angle |
| Layer 4 | 3.23 | 9.58 | 2.96 | -1.08 | 3.74 | -56.25 | 2.22 | -90.00 | 2.37 | -84.38 |
| Layer 3 | 3.30 | 2.50 | 2.99 | 2.50 | 3.13 | -50.14 | 1.93 | -31.53 | 2.06 | 8.65 |
| Layer 2 | 3.30 | 2.50 | 2.99 | 2.50 | 3.13 | -50.14 | 1.93 | -45.14 | 2.06 | 19.64 |
| Layer 1 | 3.25 | 1.08 | 2.94 | 1.08 | 3.42 | 50.63 | 2.30 | 67.50 | 2.44 | 84.38 |
| | **Increase of the average of the first torsion and bending frequencies** | | | | | | | | **4.092285** | **Hz** |
| | **Increase of the first torsion frequencies** | | | | | | | | **1.21734** | **Hz** |
| | **Increase of the first bending frequencies** | | | | | | | | **6.96723** | **Hz** |

**Table 7a and 7b. Results for Average of First Bending and Torsion Frequencies Maximization (Thickness in mm, angle in °)**

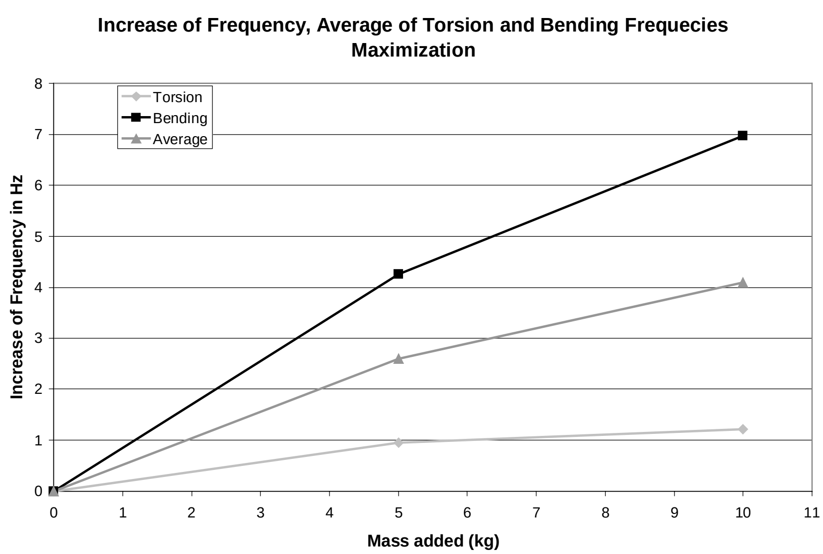


**Figure 13: Increase of Average of First Bending and Torsion Frequencies Maximization**

## 6. Weld Optimization Using Sizing Optimization

Size optimization can be utilized as an efficient method to determine the optimal locations of welds. If the structure already has welds, the procedure described here can be used to remove the least effective ones. If the welds are not in the model, this procedure requires allocating candidate welds. Once the candidate welds are located, the procedure used here is simple: wherever this is a spot weld connection, it added a new grid and a new 3d elastic element. This is done so that if the elastic element stiffness is used the connection is restored or if the elastic element is removed the connection is effectively unused. One design variable is assigned to each 3D elastic element. Given the performance requirement and a preliminary design, the iterative design cycles will lead to the search of optimal value of the design variables. The value of each design variable ranges between 0.0 and 1.0, where 1.0 indicates that the elastic element has its normal stiffness, and 0.0 indicates that the elastic element has no stiffness. The welds corresponding to the optimal value close to 1.0 are kept, and those welds corresponding to the optimal value close to 0.0 are discarded. Performance evaluation using eigenvalue analysis is used to evaluate the rigidity of the optimized model in which unnecessary welds are taken out. By using different weld constraints to study critical areas, the relation between the rigidity and quantity of welds can be determined.

In the present work, the PORSCHE 928 mesh is used as an example to describe an optimization procedure for the weld design of an automobile body. Often the lowest natural frequencies are directly related to some performance index of the structure. The first torsional frequency and first bending frequency are usually considered as rigidity indices of an automobile body. Figure 14 shows the finite element model used. The car body contains 64 fully welded parts. Eigenvalue analysis gave the first torsional frequency as 31.962 Hz and the first bending frequency as 46.185 Hz.

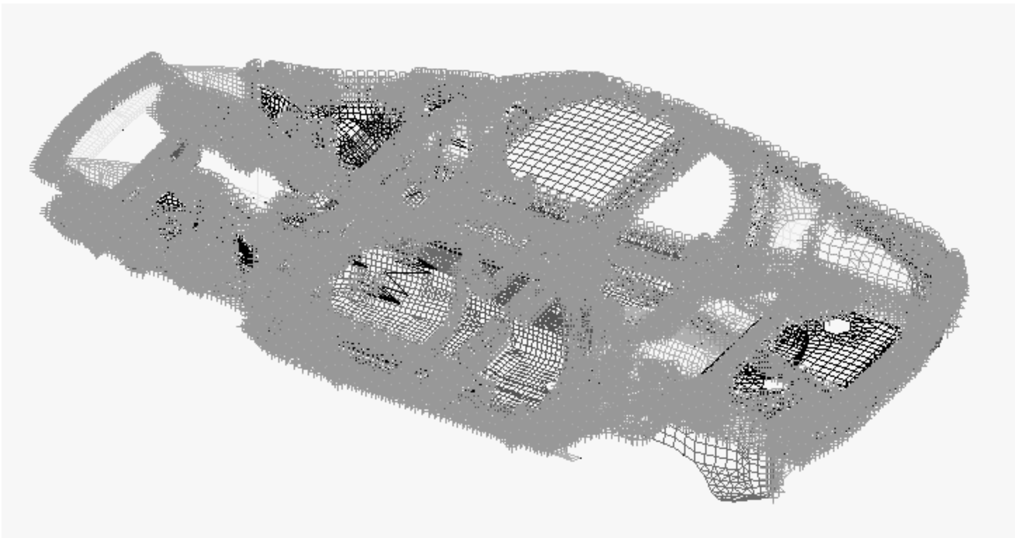

**Figure 14. Weld Optimization Model of Car Body**

The weld optimization model has 4316 rigid elements (RBE2s) to represent the weld and 4316 3D elastic elements (CVECTORs) were added to be able to perform the weld optimization process (Fig. 14). The summary of the original fully welded model and the weld optimization model is shown in Table 8.

| Item | Number | |
|---|---|---|
| | Original fully-welded model | Weld optimization model |
| Grid point | 27252 | 36842 |
| CBAR element | 34 | 34 |
| CQUAD4 element | 22072 | 22072 |
| CTRIA3 element | 12488 | 12488 |
| CVECTOR element | --- | 4316 |
| RBE2 element | --- | 4316 |
| Element property | 64 | 4380 |
| Material property | 1 | 1 |
| Degree of freedom | 163512 | 221052 |

**Table 8. Summary of Finite Element Model**

## 6.1 Weld Optimization Formulation

The objective of weld optimization is to maximize the rigidity while ensuring that the weld constraints are satisfied. The weld optimization problem is formulated as:

Maximize:

$$f(\mathbf{X}) = f_t(\mathbf{X}) + f_b(\mathbf{X}) \quad (1)$$

Subjected to

$$\frac{\sum_{1}^{n} X_i}{n} \le P_a^U \quad (2)$$

$$\frac{\sum_{1}^{n} X_i^3}{n} \ge P_c^L \quad (3)$$

$$0 \le X_i \le 1.0, \quad i = 1, \cdots, n \quad (4)$$

Where, f($\mathbf{X}$) is the objective function. $f_b(\mathbf{X})$ represents the first bending frequency and $f_t(\mathbf{X})$ represents the first torsional frequency. $\mathbf{X}$ is the vector of design variables. $X_i$ represents the ith design variable. The quantity $P_a^U$ is the upper bound of single average of all design variables, and the quantity $P_c^L$ is the lower bound of cubic average of all design variables. Constraints are imposed on cubic average of all design variables to force that the value of the design variables at the optimal solution becomes closer to either 1.0 or 0.0.

Six different cases were solved to get an idea of where welds can be removed from the original fully welded model, in order to have the least impact on the rigidity of the car body under the eigenvalue load case. For example, if the objective is to retain 60% of welds, the optimization process will take out 40% of the welds and keep the remaining 60%. Different weld constraints were used in each of the six cases as shown in Table 9.

| Case | Retained welds (%) | Constraints of design variables | |
|---|---|---|---|
| | | Average | Cubic average |
| 1 | 30 | ≤ 30% | ≥ 30% |
| 2 | 40 | ≤ 40% | ≥ 40% |
| 3 | 50 | ≤ 50% | ≥ 50% |
| 4 | 60 | ≤ 60% | ≥ 60% |
| 5 | 70 | ≤ 70% | ≥ 70% |
| 6 | 80 | ≤ 80% | ≥ 80% |

**Table 9: Weld Constraints**

## 6.2 Weld Optimization Results

The optimal solutions with 70% retained welds are shown in Figures 15, 16 and 17. The dark color represents the retained welds and the gray color represents the removed welds

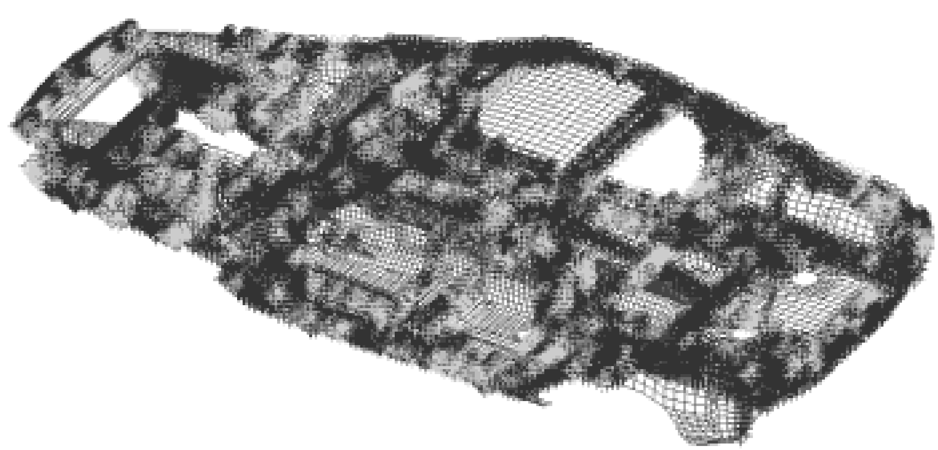

**Figure 15. Optimal Result with 70% Retained Welds and 30% Removed Welds**

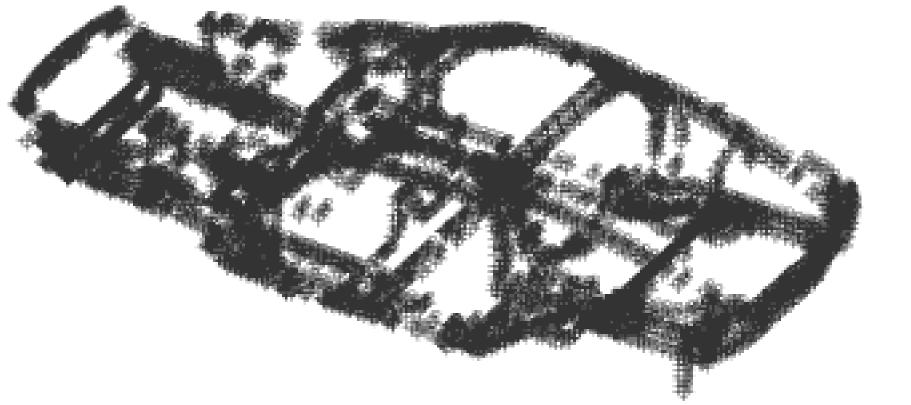

**Figure 16. Optimal Result, 70% Kept Welds**

**Figure 17. Optimal Result, 30% of Removed Welds**

### 6.3 Performance Evaluation

The optimized weld configuration was obtained from the original fully welded model after taking out the RBE2 elements corresponding to the design variables whose optimal value was found to be close to 0. Eigenvalue analysis was performed to obtain the lowest natural frequencies of the optimized model. Table 10 and Figure 18 show the relation between the rigidity and quantity of welds. Table 10 also contains the solutions for the fully welded case.

| Quantity of kept welds (%) | First torsional frequency (Hz) | First bending frequency (Hz) | Sum of two frequencies (Hz) |
|---|---|---|---|
| 30 | 24.983 | 35.100 | 60.083 |
| 40 | 26.662 | 37.330 | 63.992 |
| 50 | 29.831 | 40.755 | 70.586 |
| 60 | 30.499 | 42.100 | 72.599 |
| 70 | 31.312 | 44.947 | 76.259 |
| 80 | 31.762 | 45.718 | 77.480 |
| 100 | 31.962 | 46.185 | 78.147 |

**Table 10. Relation Between Rigidity and Number of Welds.**

\

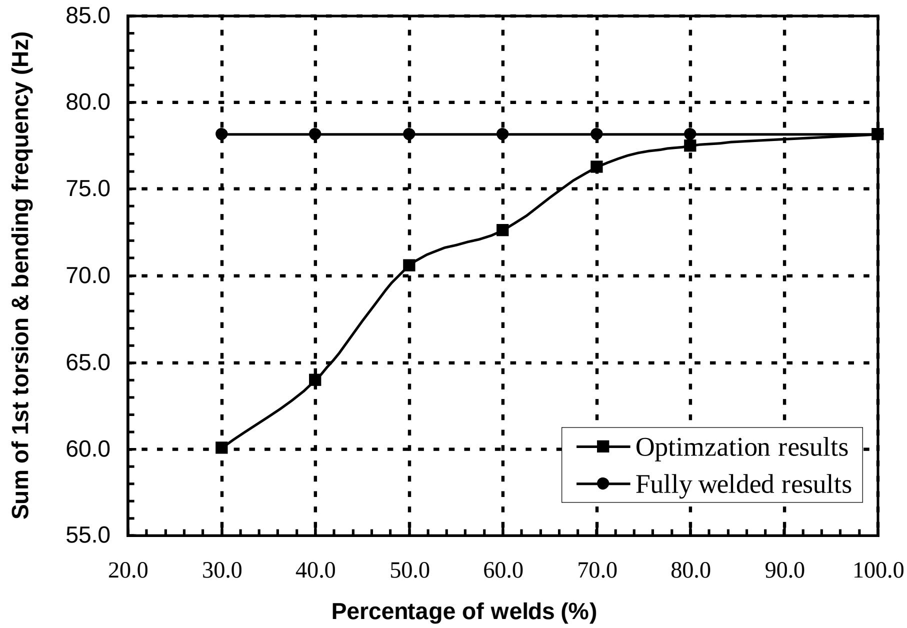


**Figure 18. Relation Between Rigidity and Number of Welds**

### 6.4 Weld Optimization Discussion

From table 10 it can be seen that if 20% welds are removed, the rigidity decreases by only 0.85% (or 0.667 Hz), which has very limited impact on the performance of the automobile body. With 30% welds removed, the rigidity drops by 2.4% (or 1.888 Hz). This table gives the designer a trade-off table to choose between the number of welds and desirable level of rigidity.

## 7. Conclusions

The GENESIS program was briefly described. Three studies were presented to show how designers could use structural optimization to improve their designs. The first study showed how topology optimization could be used to find out which regions are the most efficient regions for reinforcement. The second study showed that using sizing optimization, composite patches could be optimized to reinforce existing designs. The third study demonstrated a technique that help designers to pick up the necessary number of welds or the location of welds for the optimal design of automobile bodies while assuring the rigidity requirements are met.

## 8. References


1. *GENESIS* Structural Optimization Software, Version 6.0. User's Manual. Vanderplaats Research and Development, Inc. Colorado Springs, CO, USA, January 2000.
2. Schmit, L. A. and Farshi, B., "Some Approximation Concepts for Structural Synthesis," AIAA J., Vol. 12(5), pp. 692-699, 1974.

3. Schmit, L. A. and Miura, H., “Approximation Concepts for Efficient Structural Synthesis,” NASA CR-2552, 1976.
4. Vanderplaats, G.N. and Salajegheh, E., “A New Approximation Method for Stress Constraints in Structural Synthesis,” AIAA J., Vol. 27, No. 3, pp. 352-358, 1989.
5. Canfield, R. A., “High-Quality Approximations of Eigenvalues in Structural Optimization of Trusses,” AIAA J., Vol. 28, No. 6, pp. 1116-1122, 1990.
6. Vanderplaats, G. N., Numerical Optimization Techniques for Engineering Design; with Applications, 3rd Ed., Vanderplaats Research & Development, 1999.
7. Leiva, J.P., and Watson, B.C., “'Shape Optimization in the GENESIS Program,” Optimization in Industry II, Banff, Canada, June 6-11, 1999.
8. Leiva, J.P., Watson, B.C., and Kosaka, I., “Modern Structural Optimization Concepts Applied to Topology Optimization,” Proceedings of the 40th AIAA/ASME/ASCE/AHS/ASC Structures, Structural Dynamics, and Material Conference. St. Louis, MO, April 12-15, 1999, pp 1589-1596.
9. Bendsoe, M.P., “Optimal Shape Design as a Material Distribution Problem,” Structural Optimization Vol. 1, 1989, pp. 193-202.
10. DOT User’s Manual, Version 5.0. User's Manual. Vanderplaats Research and Development, Inc. Colorado Springs, CO, USA, January 1999.
11. Vanderplaats, G., “Very Large Scale Optimization,” presented at the 8th AIAA/USAF/NASA/ISSMO Symposium at Multidisciplinary Analysis and Optimization, Long Beach, CA September 6-8, 2000.
12. Thanedar, P.B., Sankaranarayanan, S. and Chirehdast, M., “Topology & Shape Design Optimization,” AMD-Vol. 227. Design Optimization with Applications in Industry. ASME, pp. 163-174, 1997.
13. Chen, C.J., Maire, S. and Usman, M., “Improved Fuel Tank Design Using Optimization,” AMD-Vol. 227. Design Optimization with Applications in Industry. ASME, pp. 177-188, 1997.
14. White, J.A. Jr. and Webb, J.C., “Air Cleaner Shell Noise Reduction with Finite Element Shape Optimization,” Proceedings of the Society of Automotive Engineers Noise and Vibration Conference and Exposition. Detroit, MI, USA, pp. 59, 1997.
15. White, J.A. Jr., “Practical Applications of Optimization Theory to Induction System Design,” Global Powertrain Congress, Stuttgard, Germany, October 5-6, 1999.
16. Leiva, J.P., “Structural and General Optimization Applications using VR&D Software,” LS-DYNA and Optimization Symposium on Design Optimization, Seoul, Korea, December 8-9, 2000.
17. Leiva, J.P., “Industrial Applications Using Structural Optimization with GENESIS,” 4th World Congress in Structural and Multidisciplinary Optimization, Dalian, China, June 4-8, 2001.